Modified Brayton Refrigeration Cycles for Liquid Hydrogen in Spallation Neutron Source Moderator

H.-M. Chang[1,2], S.G. Kim[1], J.G. Weisend II[2], H. Quack[3]

[1] Hong Ik University, Seoul, 121-791, Korea
[2] European Spallation Source, SE-221 00 Lund, Sweden
[3] TU Dresden, D-01062 Dresden, Germany

ABSTRACT

A thermodynamic study of standard and modified Brayton refrigeration cycles is carried out to cool liquid hydrogen in spallation neutron facilities. The target moderators under development at ESS require a refrigeration capacity of 30 kW at 20 K to remove the dissipated energy from sub-cooled liquid hydrogen. A standard Brayton refrigeration cycle to perform this refrigeration is designed with helium as refrigerant. A variety of modified processes are examined for improved efficiency and suitability. The modification includes the comparison of LP (low-pressure) and HP (high-pressure) cooling, depending on the location of cryogenic expander in the cycle, and two-stage and dual-turbine cycles, depending on the manner of combining the two expanders. Based on existing and proposed designs, eight different cycles are selected and analyzed fully with the assumed models of the components. The results are presented in terms of the figure of merit (*FOM*) as an index of the thermodynamic performance, and the detailed exergy expenditure is also investigated. As a result of this analysis, a modified dual-turbine cycle is recommended for large-capacity refrigeration at 20 K.

INTRODUCTION

Cryogenic refrigeration at 20 K is required for liquid-hydrogen moderators in spallation neutron source facilities[1-5]. As shown in Figure 1, the dissipated energy of neutrons is removed at the moderators by a circulating flow of sub-cooled liquid hydrogen at temperatures below 20 K, and then delivered to a refrigerator via a helium-hydrogen (He-H_2) heat exchanger (HX). The closed loop of liquid hydrogen can be plotted as a counterclockwise triangular cycle on the phase diagram, as shown in Figure 1. The cooling flow through the moderators is represented by a descending line according to the magnitude of the pressure drop and the temperature rise, which are restored by a pump and by the refrigerator, respectively. In order to avoid any vaporization, liquid hydrogen is maintained at a sub-cooled temperature (at 17~20 K) and at the approximate critical pressure (1.32 MPa). The refrigeration load is 1.5~6 kW for the existing systems under operation or nearing completion[1-3]. A much larger cryogenic moderator system has been recently designed and will be completed by 2019 for the European Spallation Source (ESS)[4,5], where the maximum heat load is estimated to be over 30 kW during the operation with a full level of beam power.

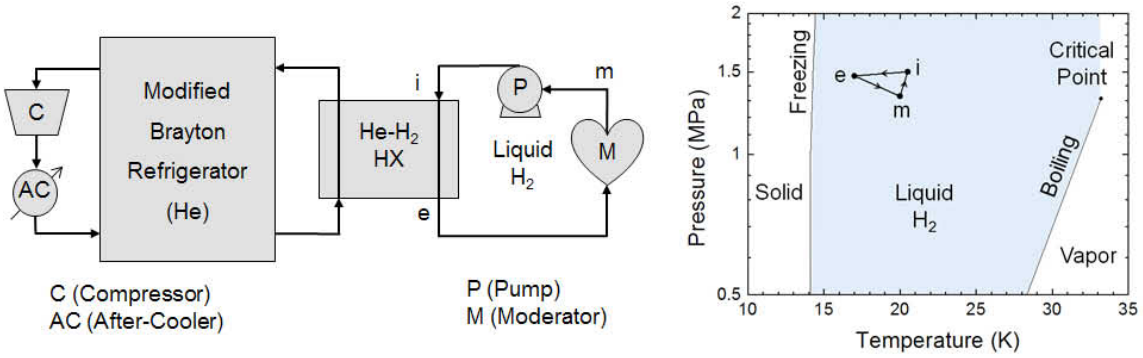

Figure 1. Cryogenic refrigeration system and liquid-hydrogen cycle on phase diagram.

The cryogenic refrigerators to cover 1.5~6 kW at 20 K have been designed as a standard reverse-Brayton cycle[1-3]. Helium is the only possible gas refrigerant for this application, as a cryogenic turbine should be used at temperatures below 20 K. The standard Brayton cycle could be modified in various ways to increase the thermodynamic efficiency and refrigeration capacity, or to satisfy other design requirements. The thermodynamic design of the 30 kW refrigerator for ESS is a new and exciting challenge at 20 K, since it requires not only the largest capacity ever, but also a set of thermo-hydraulic and geometric constraints[5]. This study investigates the structures of standard or modified cycles in a systematic way, and provides a thermodynamic basis for the development of large-scale refrigerators at 20 K.

STANDARD AND MODIFIED CYCLES

Eight different refrigeration cycles are selected and shown in Figure 2. Cycle (I) is the standard Brayton cycle that has one recuperative heat exchanger (HX1) and one expander (E) or turbine. This cycle is called "Standard cycle with LP (low-pressure) cooling", since the cold helium (state 3) enters HX2 after expansion for the thermal contact with LH_2. Cycle (II) is another simple cycle with one He-He HX and one expander, but is called "Standard cycle with HP (high-pressure) cooling", since the cold helium (state 2) enters HX2 before the expansion. The efficiency of these standard cycles has a certain limit (no matter how highly effective HX1 may be), because there is a mismatch in the specific heat of He between the HP and the LP streams.

The limit of standard cycles can be overcome by employing two expanders[6]. The first way is to arrange two expanders in series such that the first (warm) expander is used to compensate the mismatch of specific heat and the second (cold) expander plays the main role of cryogenic refrigeration. Cycles (III) and (IV) are such examples, which are called "Two-stage cycle with LP cooling" and "Two-stage cycle with HP cooling", respectively. In these two-stage cycles, the flow rate is the same for the two expanders, but the operating pressure is different.

Another way is to arrange two expanders in parallel so that they work at the same pressure level. Among a variety of possible structures, Cycles (V) and (VI) are selected, as called "Dual-turbine cycle with LP cooling" and "Dual-turbine cycle with HP cooling", respectively. At a location of the HP stream (state 2), a small fraction of gas is diverted, expanded through the first (warm) expander, and reunited with the LP stream below HX2. The main HP stream continues through HX2 and HX3, and is finally expanded through the second (cold) expander to the coldest temperature. The structure of these cycles is similar to the Claude cycle, except that the JT valve is replaced by a cold expander. In HX2, the LP stream has a higher flow rate than the HP stream in order to compensate for the mismatch in specific heat.

The cold end of the dual-turbine cycles could be further modified by adding a warm-up flow to the HP stream before entering the cold turbine, as shown in Cycles (VII) and (VIII), and called "Modified dual-turbine cycle with LP cooling" and "Modified dual-turbine cycle with HP cooling", respectively. In these cycles, the number of He-He HX's is five, and HX4 is a triple-stream HX, having two cold streams and one warm stream. The warm-up flow could be effective in reducing the temperature difference at the cold end as described later.

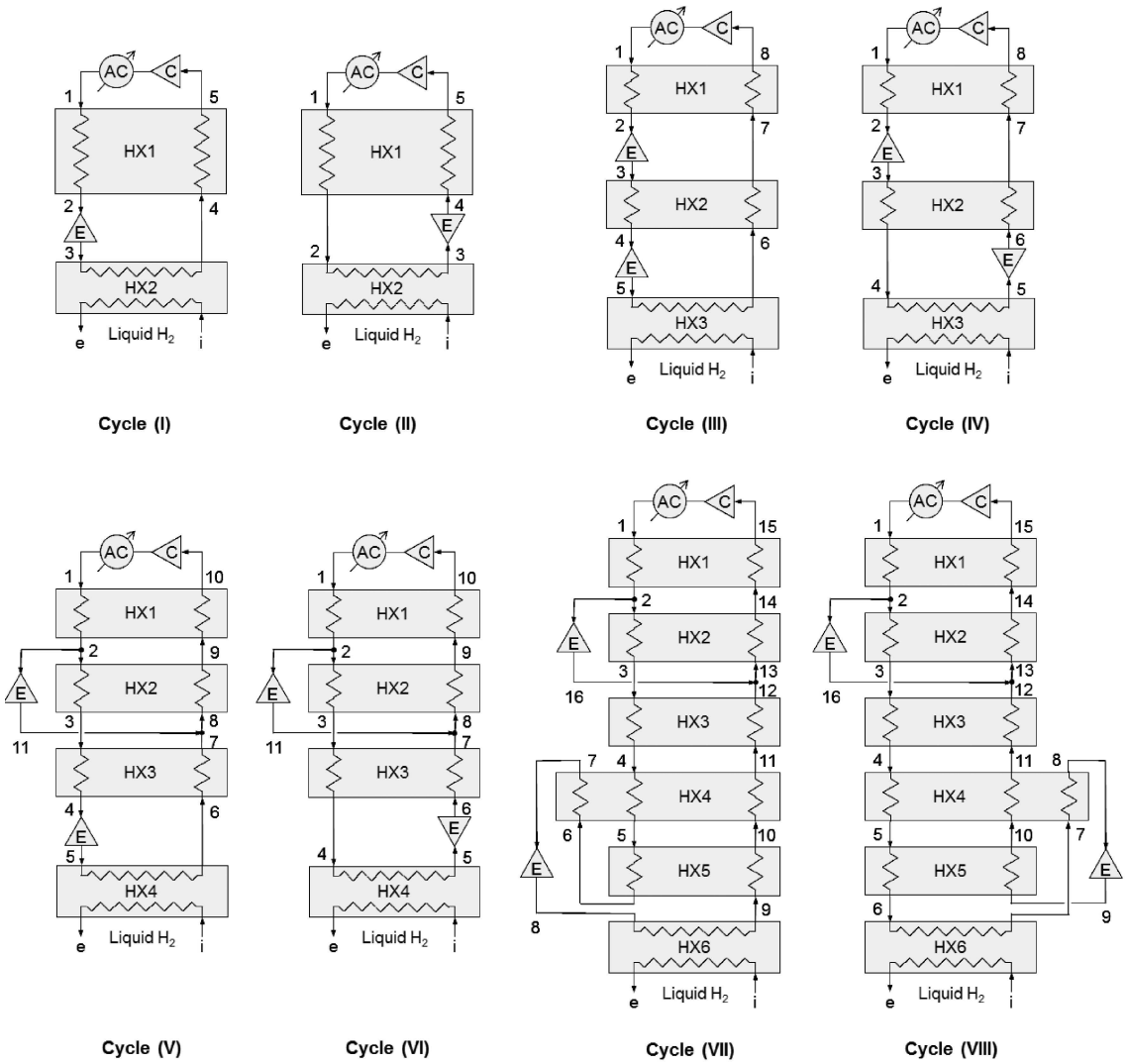

Figure 2. Standard or modified Brayton cycles for sub-cooled liquid hydrogen. (AC: after-cooler, C: compressor, HX: heat exchanger, E: expander)

CYCLE ANALYSIS

The following assumptions are made to analyze and compare the selected cycles.

- The ambient temperature (T_0) is 298 K.
- The refrigeration load by liquid hydrogen is 30 kW.

$$\dot{m}_{H_2}\left(h_i - h_e\right)_{H_2} = 30 \text{ kW} \tag{1}$$

- At the He-H_2 HX, the inlet and exit temperatures of He are 15 K and 20 K, respectively, and the pressure drop of He flow is 0.1 MPa. The minimum temperature difference between H_2 and He is 0.5 K.
- The high pressure of all cycles is 2 MPa.
- The pressure drop in all He-He HX's is zero.
- The minimum temperature difference between hot and cold streams is 3 K (or 4.5 K) for HX1, and 1% (or 1.5 %) of the absolute temperature at HP stream for other HX's.
- The adiabatic efficiency of all compressors and turbines is 80%.

The second and third assumptions are specified by the design requirements of the target moderator system at ESS[7]. The sixth assumption is made to investigate the size effect of HX's on each cycle with two different cases ($\Delta T_{\min}$ = 3 K and 4.5 K), which represents relatively high and low effectiveness, respectively. The temperature difference given as 1% (or 1.5%) of absolute temperature means, for example, that $\Delta T_{\min}$ = 1 K (or 1.5 K) at T_{HP} = 100 K and $\Delta T_{\min}$ = 0.4 K (or 0.6 K) at T_{HP} = 40 K. Since the temperature of the HP stream is determined as a result of the cycle analysis,

this assumption will be imposed by a few iterative calculations. In calculating the input power to the compressors, a single-stage compression is assumed, because the pressure ratio is between 3 and 7 and screw compressors could be used in practice. The only exception is Cycle (II), where a two-stage compression with inter-cooling is assumed for the pressure ratios exceeding 10.

A general-purpose process simulator (Aspen HYSYS®) with the thermodynamic properties of helium and para-hydrogen is used for the cycle analysis. Under the specified conditions, Cycles (I) and (II) are uniquely determined, as the number of unknowns is the same as the number of given equations. For Cycles (III) through (VIII), however, the number of unknowns is more than the number of given equations by one. The cycle analysis is repeated over one variable, until the input power can be minimized under the assumptions.

The thermodynamic performance of a refrigeration cycle is evaluated with a dimensionless index, *FOM* (the figure of merit)[8], which is defined as the ratio of minimum to the actual work.

$$FOM = \frac{\dot{W}_{\min}}{\dot{W}_C - \dot{W}_E} \tag{2}$$

The minimum work is the thermodynamic limit for a reversible cycle, which can be expressed as the increase of exergy or flow availability of liquid hydrogen.

$$\dot{W}_{\min} = \dot{m}_{H_2}\left[\left(h_e - h_i\right)_{H_2} - T_0\left(s_e - s_i\right)_{H_2}\right] = 447.0 \text{ kW} \tag{3}$$

where h and s are specific enthalpy and entropy, respectively. The subscripts e and i denote the exit and inlet of He-H_2 HX, respectively, as shown in Figure 1 and 2, and T_0 is the ambient temperature at which heat is rejected by the refrigerator. In practice, the power output of the expanders (W_E) may be used to drive the compressors or may be simply dissipated, but the "net" input (W_C - W_E) is counted in the denominator of Eq. (2).

For a better understanding of the thermodynamic nature of cycles, an exergy (or second-law) analysis is presented as well. Combining the energy and entropy balance equations[9], the exergy balance can be written as:

$$\dot{W}_C - \dot{W}_E = \dot{W}_{\min} + T_0\left[\left(\dot{S}_{gen}\right)_C + \left(\dot{S}_{gen}\right)_{AC} + \left(\dot{S}_{gen}\right)_E + \sum_{HX}\left(\dot{S}_{gen}\right)_{HX}\right] \tag{4}$$

where the left-handed side is the exergy input for refrigeration, and the right-handed side shows so-called the exergy expenditure. As defined in Eq. (2), the fraction of the first term is the *FOM*, and the remaining terms are the irreversibility or the entropy generation rate multiplied by ambient temperature. The total irreversibility can be itemized for the components in the system, including compressors (C), after-coolers (AC), expanders (E), and heat exchangers (HX). In case of Cycles (IV) through (VIII), the mixing of two streams is another source of entropy generation, but is not included here, since the magnitude is negligibly small for an optimized cycle[10].

RESULTS AND DISCUSSION

The selected eight cycles are fully analyzed with the assumptions described above, and the results are plotted as temperature-entropy diagram in Figure 3 and exergy expenditure in Figure 4. The cycles with $\Delta T_{\min}$ = 3 K (1%) are presented here, and will be discussed later together with $\Delta T_{\min}$ = 4.5 K (1.5%). As mentioned above, Cycles (III) through (VIII) have been optimized for the maximum *FOM*.

In the case of the standard cycles, Cycle (I) with LP cooling is more efficient than Cycle (II) with HP cooling. The main reason is that the HP cooling needs a larger pressure ratio to perform the refrigeration. The pressure ratio is 6.9 and 19.7 in Cycles (I) and (II), respectively. In a sense, the HP cooling is regarded as "indirect" cooling, because the coldest LP stream cools the HP stream, and then the HP stream cools the LH_2 flow. It may be stated in standard cycles that the LP cooling is essentially superior in efficiency to the HP cooling. On the other hand, the HP cooling could have merits in other aspects, such as a smaller diameter of transfer lines for cold helium. The HP cooling could also be safer against the freeze-out of liquid hydrogen, because the coldest helium (at the exit of turbine) indirectly affects the LH_2 flow, when the temperature temporarily drops according to a scheduled or unscheduled decrease of thermal load.

Two-stage cycles, Cycles (III) and (IV), have considerably higher *FOM's* than the standard cycles. In Figure 4, the irreversibility in HX's of Cycles (III) and (IV) is smaller than that of Cycles

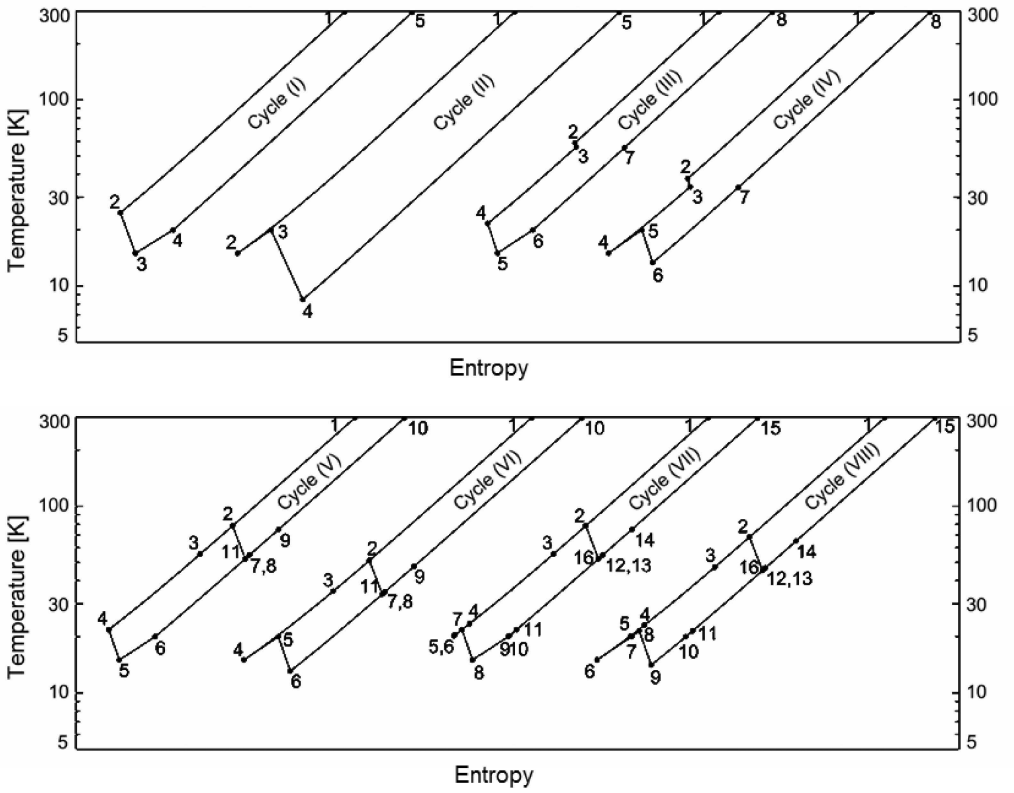

Figure 3. Temperature-entropy diagram of eight cycles at optimized condition with $\Delta T_{\min} = 3$ K (1%).

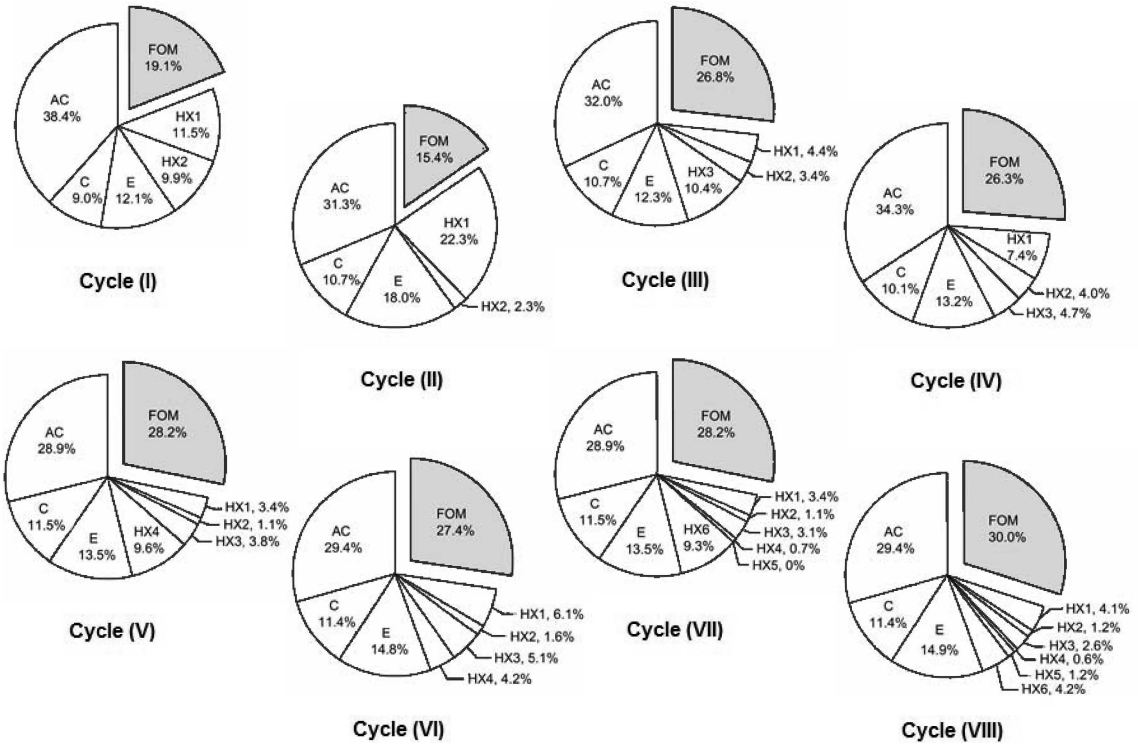

Figure 4. Exergy expenditure of eight cycles at optimized condition with $\Delta T_{\min} = 3$ K (1%). (FOM: figure of merit, AC: after-cooler, C: compressor, E: expander, HX: heat exchanger)

(I) and (II), as the temperature difference in HX's is reduced by the addition of warm expander. A key point here is that the LP cooling is still more efficient than the HP cooling, but their difference in *FOM* is not so large. It is interesting to notice in Figure 4 that Cycle (IV) has a larger irreversibility in HX1+HX2 than Cycle (III), but a smaller irreversibility in HX3. This means that the HP cooling still requires a larger pressure ratio (for a larger temperature difference), but the penalty of

pressure drop (0.1 MPa) in HX3 is less severe in HP cooling. The pressure ratio is 4.7 and 5.3 for Cycles (III) and (IV), respectively.

The dual-turbine cycles, Cycles (V) and (VI), have an even higher *FOM's* than the two-stage cycles. The branching flow through the warm turbine is effective in reducing the temperature difference in recuperative HX's, and the pressure ratio is small for both cycles. Like typical Claude cycles, the main design parameter is the ratio of the flow rate through the warm turbine to the total flow rate through the compressor[8]. The optimal condition is determined such that the exit temperature of the warm turbine (state 11) matches closely with the LP temperature at the point of mixing. The flow ratio is 0.114 and 0.210 for Cycles (V) and (VI), respectively, and the pressure ratio is 3.9 and 4.0 for Cycles (V) and (VI), respectively.

The modification of dual-turbine cycle with a warm-up flow is not as effective in improving the *FOM* for LP cooling, but is very effective for HP cooling. Cycles (VII) has nearly the same *FOM* as Cycle (V), even though the detailed cycles are slightly different from each other. On the other hand, Cycle (VIII) has a significantly higher *FOM* than Cycle (VI). Two additional HX's at the cold end and the warm-up flow make the operating temperature of the warm turbine higher and accordingly the overall temperature difference in the HXs is smaller. The flow ratio to the warm turbine is 0.114 and 0.136 for Cycles (VII) and (VIII), respectively, and the pressure ratio is 3.9 and 4.0 for Cycles (VII) and (VIII), respectively.

In order to examine the size effect of the HXs, Figure 5 compares the *FOM* of eight cycles with the minimum temperature difference of 3 K (1%) and 4.5 K (1.5%). The standard cycles, Cycles (I) and (II), are not only poor in efficiency itself, but also more sensitive to the size of HXs than the modified cycles. Among the modified cycles, dual-turbine cycles are superior to two-stage cycles, if highly effective HXs are used. The penalty of small HX size is least for Cycle (VIII). This means that an efficient refrigeration with HP cooling can be achieved by the warm-up flow without an extremely large size of HXs.

In summary, two cycles are suggested from a thermodynamic point of view. First, the dual-turbine cycle with LP cooling or Cycle (V) is a preferred cycle for both simplicity and efficiency. This cycle is especially recommendable when highly effective HXs can be used. Alternatively, the modified dual-turbine cycle with HP cooling or Cycle (VIII) has an advantage in efficiency, even when the HXs are not so highly effective. On the other hand, this cycle is complex in structure and could yield more pressure drops in the HXs. Table 1 lists the detailed thermodynamic data, including temperature, pressure and flow rate at each state for Cycle (V) with ΔT_{min} = 3 K (1%) and Cycle (VIII) with ΔT_{min} = 4.5 K (1.5%).

In determining a refrigeration cycle, there are a number of practical factors to take into account as well as efficiency. Although the details are beyond the scope of this thermodynamic study, a few comments are mentioned for discussion. First, the availability and performance of cryogenic turbines should be considered for the selection between the two-stage cycle and the dual-turbine

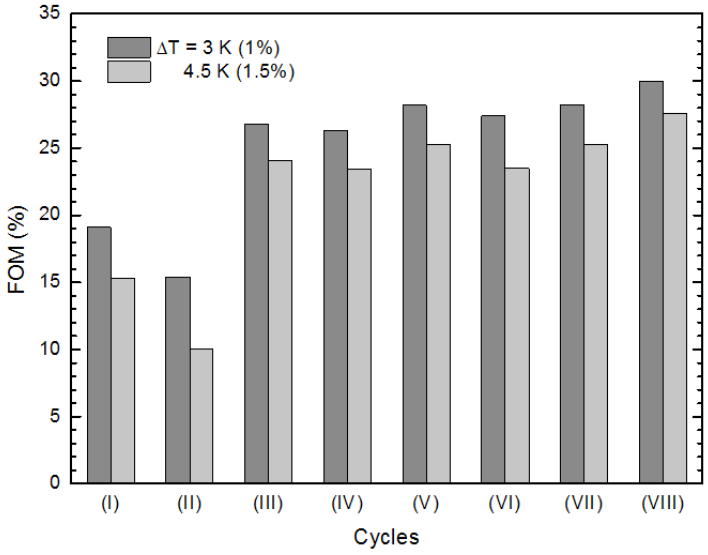

Figure 5. Figure of merit (FOM) for eight cycles with ΔT_{min} = 3 K (1%) and 4.5 K (1.5%).

Table 1. Temperature, pressure and flow rate of two suggested cycle

		1	2	3	4	5	6	7	8	9	10	11	12	13	14	15	16
Cycle (V)	T [K]	298.0	78.5	55.4	21.8	15.0	20.0	54.9	54.6	75.3	295.0	52.3					
	P [MPa]	2.00				0.61	0.51										
	m [kg/s]	1.18		1.04					1.18			0.14					
Cycle (VIII)	T [K]	298.0	85.7	57.5	23.9	20.3	15.0	20.0	21.9	14.0	20.0	21.9	56.7	56.5	81.0	293.5	55.2
	P [MPa]	2.00						1.90	0.50								
	m [kg/s]	1.09		0.94									1.09				0.15

cycle. In two-stage cycles, the warm turbine requires a small pressure ratio with a large flow rate. In dual-turbine cycles, on the contrary, the warm turbine requires a large pressure ratio with a small flow rate.

Detailed HX design could be important for a thorough and fair comparison of the cycles. It is recalled that the results presented are based on a simplified model of minimum temperature difference and an assumption of no pressure drop in the HXs. The actual size and thermo-hydraulic characteristics of the HXs could affect the selection to an extent. Finally, an optimization theory is cited here with regards to the effect of finite HX sizes, especially when a cycle is composed of multi-stages of HXs. It is always true that as any HX area increases, the temperature difference between hot and cold streams in the HX decreases. It is an important design strategy, however, to allocate the HX area to each stage, if the total sum of HX area is fixed. This is a well-known optimization problem subject to a constraint, which has been solved by the method of Lagrange multiplier. The results show that the best thermodynamic performance is achieved when the temperature difference is proportional to the absolute temperature[9,11].

$$\left(\frac{\Delta T}{T_{HP}}\right)_{\text{opt}} \approx \text{constant} \tag{5}$$

This condition has been already incorporated as an assumption of the cycle analysis.

CONCLUSIONS

Standard and modified Brayton refrigeration cycles are investigated, with an aim at the efficient refrigeration of 30 kW for sub-cooled liquid hydrogen at 20 K. Based on existing and proposed systems, a variety of modifications are tried in a systematic way, and their efficiency is calculated in terms of *FOM* (figure of merit) through a full thermodynamic analysis. The modifications include the LP (low-pressure) or HP (high-pressure) cooling, depending on the location of the cryogenic expander in a cycle, and the two-stage or dual-turbine cycles, depending on the combination of the two expanders. Among the eight cycles under consideration, two cycles are suggested along with the required size of HXs and other constraints. A dual-turbine cycle with LP cooling or Cycle (V) is preferred for simplicity and efficiency at the same time, if highly effective HXs can be used. A modified dual-turbine cycle with HP cooling or Cycle (VIII) has an advantage in efficiency, even if less effective HXs are used. The results of this thermodynamic study are immediately applicable to the neutron source moderators at ESS, and should be useful in large-scale refrigeration at 20 K as well.

ACKNOWLEDGMENT

This work was partially supported by 2016 Hong Ik University Research Fund for sabbatical leave in a foreign institute.

REFERENCES

1. Aso, T., Tatsumoto, H., Hasegawa, S., Ushijima, I., Kato, K., Ohtsu T., Ikeda, Y., "Design result of the Cryogenic Hydrogen Circulation System for 1 MW Pulse Spallation Neutron Source (JSNS) in J-PARC," *Adv. in Cryogenic Engineering*, Vol. 51, Amer. Institute of Physics, Melville, NY (2006), pp. 763-770.
2. Lee, M., Choi, H.Y., Han, J.S., Cho, S.H., Kim, M.S., Hur, S.O., Son, W.J., Ahn, G.H., Lim, I.C., "Operational characteristics of the helium refrigeration system at HANARO-CNS," *Adv. in Cryogenic Engineering*, Vol. 57, Amer. Institute of Physics, Melville, NY (2012), pp. 361-367.
3. Wang, G.P., Zhang, Y., Xiao, J., He, C.C., Ding, M.Y., Wang, Y.Q., Li, N., He, K., "Design progress of cryogenic hydrogen system for China Spallation Neutron Source," *Adv. in Cryogenic Engineering,* Vol. 59, Amer. Institute of Physics, Melville, NY (2014), pp. 233-238.
4. Arnold, P., Hees, W., Jurns, J., Su, X.T., Wang, X.L., Weisend, J.G., "ESS cryogenic system process design," *IOP Conference Series: Materials Science and Engineering* Vol. 101, No. 1 (2015), IOP Publishing, p. 012011
5. Jurns, J., Ringnér, J., Quack, H., Arnold, P., Weisend, J.G, Lyngh, D., "Spallation target cryogenic cooling design challenges at the European Spallation Source," *IOP Conference Series: Materials Science and Engineering* Vol. 101, No. 1 (2015), IOP Publishing, p. 012082.
6. Chang, H.M., Park, J.H., Cha, K.S., Lee, S., Choe, K.H., "Modified Reverse-Brayton Cycles for Efficient Liquefaction of Natural Gas," Cryocoolers 17, ICC Press, Boulder, CO (2013)„ pp. 435-442.
7. European Spallation Source, *Annex 4 Technical Specification*, Document Number ESS-0034501 (2015), pp. 41-42.
8. Barron, R. F. *Cryogenic Systems*, Clarendon Press, 1985, pp.237-261.
9. Bejan, A., *Advanced Engineering Thermodynamics*, 3rd ed., John Wiley & Sons, New Jersey (2006), pp. 101-142.
10. Chang, H.M., Lim, H.S., Choe, K.H., "Thermodynamic design of natural gas liquefaction cycles for offshore application," *Cryogenics*, 63 (2014), pp. 114-121.
11. Chang, H.M., Chung, M.J., Lee, S., Choe, K.H., "An efficient multi-stage Brayton-JT cycle for liquefaction of natural gas," *Cryogenics*, 51, no. 6 (2011), pp. 278-286.